Version 1.3
based on LHCb-PUB-2015-005

Measurement of matter-antimatter asymmetries with the LHCb experiment

TU Dortmund University,
AG Albrecht

14th April 2022

Abstract

This document contains an instruction for the data analysis lab experiment of the AG Albrecht. The analysis is performed as part of the specialisation course "Particle physics and detectors". The goal is to understand and measure the differences in the behaviour of matter and antimatter with data recorded by the LHCb experiment. For this purpose, three-body decays $B^{\pm} \to h^{\pm}h^{+}h^{-}$, in which the hadrons $h^{\pm}$ are either pions $\pi^{\pm}$ or kaons $K^{\pm}$, will be studied. The analysis includes the measurement of both inclusive matter-antimatter asymmetry and larger asymmetries in local regions of the phase space.

1 Aims & guidelines for the analysis

Basic knowledge of special relativity and of the quark model are required for this analysis. However, no in-depth knowledge of particle physics is assumed. The programming language Python is used for the implementation. Previous knowledge of Python is helpful, but not assumed. There are sufficient examples to explain the necessary implementations. The following goals are to be achieved:

1. Understand how a detector in particle physics works
2. Understand how matter-antimatter differences can be observed
3. Understand and use of basic data analysis techniques at modern particle physics experiments
4. Write a (Python) program to select and analyse three-body decays of charged B mesons
5. Use real LHCb data to observe matter-antimatter diffferences
6. Use real LHCb data to observe intermediate resonances

2 Introduction

The Large Hadron Collider [1] (LHC) is a particle accelerator at CERN, the european organisation for nuclear research, close to Geneva. The data to be analysed in this project come from collisions of two proton beams accelerated at LHC to a centre-of-mass energy of 7 TeV. Each of these beams consists of about 2000 bunches, each containing about 1.1×10^{11} protons. These bunches have been brought into collision within the LHCb detector at an average rate of 15 MHz. In each of these collisions, called an event, there is a high probability that one or more protons from the bunches will collide. These are inelastic interactions between the components of the colliding protons.

The first data taking period (Run 1) for the physics programme at the LHC started in 2010 and ran until early 2013. It is planned that the LHC will continue to operate for another two decades, receiving a large number of upgrades. The main goal of the LHC experiments is to test the Standard Model (SM) of particle physics and to search for phenomena not described by the SM.

LHCb [2] is one of the four main experiments at the LHC. This experiment is designed to study the differences of matter and antimatter (CP violation) and rare decays of hadrons from b and c quarks. The design of the detector is described in more detail in section 4. In this project, data recorded at the LHCb experiment are used to observe CP violation. Due to the rarity of the processes to be observed, the information is obtained through statistical analysis of the large amounts of data. The data available for this analysis project has been recorded by the LHCb experiment and has already been pre-selected to only provide events of interest.

3 CP violation (CPV)

Matter-antimatter asymmetry is one of the most important unexplained phenomena in physics. Equal amounts of matter and antimatter are expected to have been created in the Big Bang. However, our present universe consists mainly of matter. A fundamental difference in the behavior of matter and antimatter, the *CP* violation, is one of the effects known as Sakharov conditions to explain this asymmetry [3].

The *CP* symmetry is the product of two symmetries: the charge inversion C, which describes the transition of particles into their antiparticles, and the space coordinate mirroring parity P. A violation of this *CP* symmetry has been discovered in 1964 [4] in weak decays of kaons. The Nobel Prize was awarded for this discovery in 1980. A mechanism to describe *CP* violation in the SM (by the CKM matrix [5]) has been proposed in 1973. The description by this mechanism was verified between 1999 and 2010 [6] by studies of *CP* violation in weak decays of B mesons at the BaBar and Belle experiment and subsequently awarded the Nobel Prize in 2008. Further information on *CP* violation can be found in the literature [7, 8].

The LHC experiments discovered in 2012 [9, 10] the Higgs boson, the last particle postulated by the SM, and are now concerned with precision tests of the SM and with the search for New Physics beyond the SM. The SM of particle physics does contain *CP* violation, but the magnitude of this effect in this one is clearly too small to explain the observable matter-antimatter imbalance in the universe. Therefore, there must be other origins of *CP* violation. Many models describing New Physics beyond the SM include new sources of *CP* violation. Therefore, precise measurements of *CP* violation are an important technique for the search for New Physics, since discrepanies between SM predictions and the result of measuremnts could hint for it. Moreover, possible discoveries of New Physics could answer other fundamental unanswered questions in physics, such as the nature of Dark Matter.

The *CP* violation can be studied experimentally by comparing the decays of particles and antiparticles. The LHCb experiment is specifically designed for such studies in the B meson region and has already provided substantial results. The regularly updated highlights of the LHCb physics program are described on the LHCb public webpage [11, 12]. The analysis to be performed in this project is based on the largest *CP* violation effects observed on the Run 1 dataset [13, 14].

4 Detector, software and data

The following description of the LHCb experiment corresponds to the status relevant to this analysis project during the first data-taking period. The LHCb detector [2, 15] is a single-arm forward spectrometer and is shown in Figure 1. A right-handed coordinate system is used for description. Here, the z-axis is along the beams into the detector and the y-axis is vertical. The negative (positive) z-region of the detector is referred to as upstream (downstream). At the LHC, the particles LHCb wants to study are produced with a strong boost in the forward direction along the direction of the proton beams. The decay products of these particles can be observed at a polar angle of $15-300$ mrad at the detector. Hadrons with b quarks travel a few millimeters to a few centimeters and decay afterwards in the detector. Therefore, as shown in Figure 2, they are reconstructed from their individual decay products.

The detector contains a high-precision tracking system for detecting charged particles. A silicon strip vertex detector, known as vertex locator (VELO) [17], surrounds the interaction region and measures at least three (usually about 10) points of each particle track with the different sensor planes in the VELO. This enables the possibility to reconstruct the position of the proton-proton interaction, the primary vertex (PV), and to determine the decay location of the b hadron. Charged particles traveling through the silicon create electron-hole pairs, which drift through the silicon in an electric field producing a signal. A large-area, four-layer silicon strip detector, known as a TT, is located in front of the dipole magnet. In the magnetic field of the dipole magnet with an integrated field strength of about 4 Tm, the trajectories of charged particles are bent. The polarity of the magnetic field is regularly reversed. In this way, systematic uncertainties are captured, which originate from the fact that different charged particles are deflected in different directions and thus into differently efficient detector regions. This strategy allows to detect detector defects from e.g. non working electronics. Three additional tracking stations (T1, T2 and T3) are located behind the magnet. These consist of four-layer silicon strip detectors and drift tubes [18]. The drift tubes are filled with gas (Ar & CO_2), which is ionized by the charged particles passing through. The ions generated in the gas drift through the tubes and generate a signal.

All these individual detector signals are combined to reconstruct the track of charged particles. The momentum p of a charged particle can be determined by the curvature of the track in the magnetic field. The complete tracking system can measure momentum with a relative uncertainty of 0.5 % at low momentum and up to 1 % at 200 GeV/c. Impact parameters (cf. 5.3 section) can be measured for charged particles with large transverse momentum p_{T} with a resolution of 20 µm.

Different types of charged hadrons (pions, kaons, and protons) are distinguished using information from the two ring-imaging Cherenkov (RICH) detectors [19]. In these detectors, particles travel through volumes of gas (CF_4, C_4F_{10}) or of ultra-light solids (aerogel). When particles pass through the Cherenkov detectors with a velocity higher than the speed of light in the detector's media, they radiate photons in the forward direction. This phenomenon is known as the Cherenkov effect. The emitted photons are detected and the angle of emission is reconstructed. This angle is directly related to the velocity of a particle. By combining the velocity information obtained with the momentum information, the particle mass can be determined and thus the particle type can be determined.

Photons, electrons and hadrons are identified with the calorimeter system. It consists of a Scintillating Pad (SPD) and a Preshower (PS) detector, an electromagnetic calorimeter (ECAL) and a hadronic calorimeter (HCAL). The calorimeters consist of alternating layers of iron (lead) and scintillators. Particles interact with the iron (lead) and are absorbed, while emitting the absorbed energy through photons. From the amount of scintillation

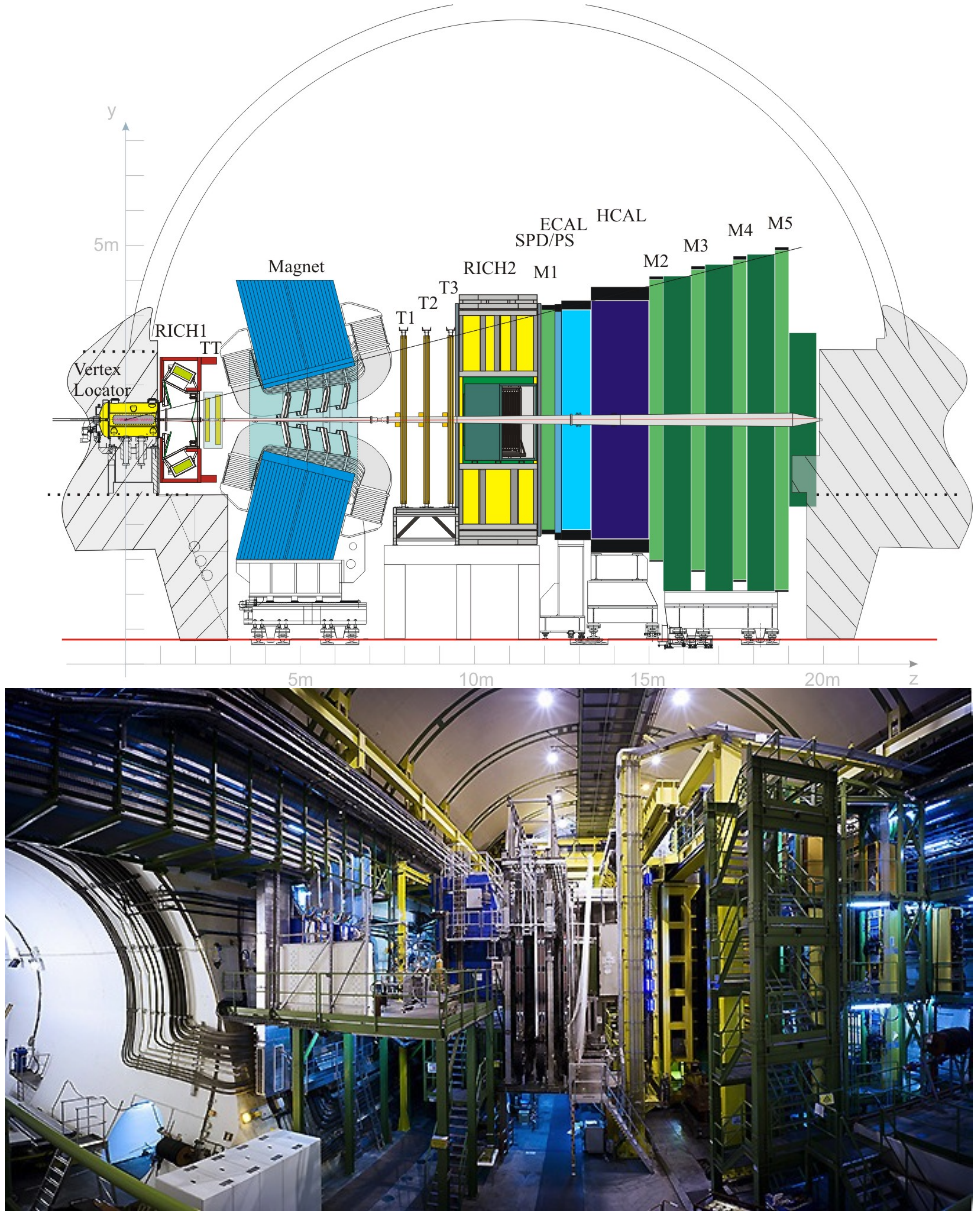

Figure 1: (Top) Layout of the LHCb detector. The beams pass horizontally through the beam pipe in the center of the detector and cross in the vertex locator on the left side of the graph. The individual components are explained in the text. (Bottom) Photograph of the LHCb cavern. The image has been mirrored to match the upper graphic.

light detected, the energy of the particles can be reconstructed. Photons and electrons are mainly absorbed in ECAL, while hadrons are mainly absorbed in HCAL. This is a result of the different interaction lengths of the different particles. Only neutrinos, which are not detected at all, and muons usually pass through the calorimeters. The muons are

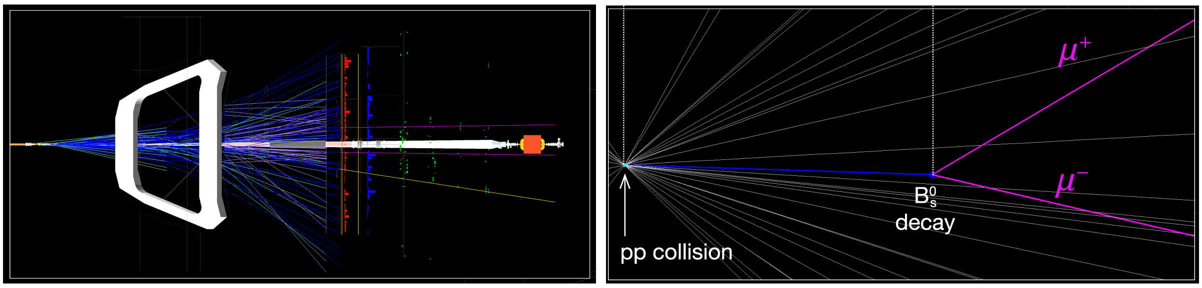

Figure 2: Event display showing the tracks of a reconstructed $B_s^0 \to \mu^+\mu^-$ candidate. The first hint of this decay [16] was one of the first significant results of the initial LHC data taking phase, as it provides strong constraints for New Physics in Supersymmetry models. (Left) All tracks reconstructed in the LHCb detector for one event. (Right) The VELO region showing the reconstructed primary vertex and secondary vertex of the decaying B_s^0 meson with a separation of 14 mm. The reconstructed muon tracks are colored magenta.

identified by a system of iron absorber layers and multi-wire chambers [20].

During the recording of the data used here, one (or more) simultaneous inelastic interactions between protons of two bunches took place at an average rate of about 11 MHz. Because of the data size of a single event recorded by the LHCb detector, the events can only be stored at a rate of 3 kHz. The system used to determine which events are stored is called a trigger [21]. It consists of a hardware implementation, based on information from the calorimeter system and the muon system, followed by a software implementation in which the event is fully reconstructed. The software implementation is run on a large farm of multiprocessor CPUs running 26 110 copies of the program. The triggers are designed to select decay channels of interest with high efficiency while discarding events of low interest.

The obtained data are then processed on a globally networked computer system, the GRID. In the process, events of interest are selected for specific physical processes. Individual groups of analysts also write programs through which further selections are made and the data size is significantly reduced by selecting relevant observables only. The data available for this analysis project have already gone through this step.

For the comparison with data, simulations are generated that can be used to investigate background processes or even the actual physical process. These also contain detailed simulations of the detector response, so that the simulated data can be directly compared with the real data. However, only simplified simulation data are available for this analysis, i.e. only the physical process was generated, but not the interaction with the detector.

The available data have been selected by the trigger system and by offline selections from the approximately 10×10^{14} collisions at LHCb in 2011. The data sample contains only the most relevant observables for this analysis to reduce the data size and runtime of the analysis project. In total, about 3.4 million (5.1 million) events with the "up" ("down") polarity of the magnet are included in the data, corresponding to an integrated luminosity of 434 pb^{-1} (584 pb^{-1}).

5 Strategy

The analysis performed here compares the rates for the decays $B^+ \to h^+h^+h^-$ and its antiparticle equivalent $B^- \to h^-h^-h^+$, where $h^\pm$ is a pion $\pi^\pm$ or kaon $K^\pm$. The B^+ mesons are composed of a $\overline{b}$ quark and u quark. The pion π^+ is composed of $\overline{d}$ and u quarks, the kaon K^+ of u and $\overline{s}$ quarks. The decays studied proceed through the weak force (via $W^\pm$ bosons), where the *CP* symmetry is known to be violated.[1]

First the decay $B^+ \to K^+K^+K^-$ should be studied. For other options

- $B^+ \to \pi^+K^+K^-$
- $B^+ \to K^+\pi^+\pi^-$
- $B^+ \to \pi^+\pi^+\pi^-$

feynman diagrams of the same order can also be drawn, but these decays are more difficult to handle experimentally due to higher background level.

The analysis can be performed on one of the interactive analysis machines of the AG Albrecht. A python notebook is provided to guide through the analysis steps. By using the `pyRoot` library, it is possible to use the CERN software package `ROOT` [22] for the analysis. The data is already on the analysis maschine. These are in the file format common to LHC experiments, with the extension `.root`. Often files of this type are called *tuple*. In this project, there are three different tuples. One contains simulated data for the decay $B^\pm \to K^\pm K^+K^-$. The other two contain data recorded by the LHCb experiment in 2011 reconstructed with a decay $B^\pm \to h^\pm h^+h^-$. The two real data sets differ in this respect by the polarity of the magnet at which the data were recorded. The number of observables available in the data sets has been reduced to a small set of variables essential to this analysis for clarity.

[1] The observation of *CP* Violation requires interference between two decay routes to the same final state.

5.1 First steps

Real data contain both the events to be observed, the signal, and a background component that could not be distinguished from the signal during the reconstruction in the trigger. Therefore, it is useful to first become familiar with the simulated data. The simulated data presented here contain only signal events and are not distorted by detector resolution effects. Therefore, the behavior of the data is completely known and can be used to check one's own approach.

After the (simulated) data have been read in, an overview of the data is to be obtained. To get an overview of the value ranges and the distributions, a table can be created. However, due to the size of the data and the number of observables, it makes more sense to create histograms for the distributions of the individual variables.

> Tasks:
>
> 1. Read and access the simulation data.
> 2. Get familiar with the data.

5.2 Reconstruction of the invariant mass

The invariant mass is a characteristic property of a particle. The mass is useful to identify a particle or distinguidh between signal and background. From special relativity the Energy-momentum relation follows

$$E^2 = (pc)^2 + (mc^2)^2. \tag{1}$$

By using the natural units[2]. this equation can be simplified as

$$E^2 = p^2 + m^2. \tag{2}$$

It can be seen from the energy-momentum relation that with known energy and known momentum the mass of a particle can be calculated. Due to momentum and energy conservation, these quantities can be identified for the B mesons as the sum of the energies and momentums of the daughter particles. The momentum of the daughter particles are quantities measured by the detector and are included in the data. This is not the case for the energy. Therefore, the energy must be calculated again via the energy-momentum relation from the measured momenta and the known masses of the daughter particles.

[2]that are common in particle physics, the speed of light c, Planck's effective quantum $\hbar$, Boltzmann's constant k_{B}, and the electric field constant ε_0 are set to the value 1. This allows all arbitrary units to be written in powers of the energy unit, usually electron volts eV

Tasks:

1. Look up the kaon mass.
2. Calculate the energy of the kaons.
3. Calculate the invariant masses and all measures of the B^+ mesons to do so.
4. Create a histogram showing the distribution of the invariant B^+ mass in the simulated data. Does the distribution meet your expectations?

5.3 Selection

So far only simulated data have been considered, where it was known that the data originate from the decay $B^\pm \to K^\pm K^- K^+$. Now, the real data will also be used where this is not the case. Therefore, a preselection of the data for the decay $B^\pm \to h^\pm h^+ h^-$ has been applied to the data first. This is done to significantly reduce the background events that do not originate from such a decay. The main cuts applied in the preselection are listed in Table 1 and explained below.

- *Momentum.* The three final state tracks should all have significant momentum (p) and momentum in the plane transverse to the beam direction (p_T) as they originate from a B decay. Tracks from background processess will typically have lower momenta.
- $B^\pm$ *Mass.* The mass of the $B^\pm$ candidate computed from the measured momenta of the final state particles (under the assumption they are kaons or pions) and events should be close to the known mass of B^+ particle.
- *Impact Parameters.* The $B^\pm$ meson has a mean lifetime τ of 1.6×10^{-12} s [23]. Therefore, it travels a distance $\gamma c \tau$ within the detector before decaying. Here γ refers to the Lorentz factor of special relativity. With in the LHCb experiment this distance is typically a few millimeter to centimeter. The distance between the primary vertex (PV), and the decay vertex (secundary vertex (SV)) into the three final state tracks is a key feature to identifying B decays. The closest distance of the extrapolated final state tracks to the primary vertex is known as the impact parameter (IP). These finale state tracks of B decays therefore will have a significant IP. The IPχ^2 is the IP divided by its estimated uncertainty all squared. Background tracks, that originate directly from the PV, therefore typically have lower χ^2_IP.

No selection has yet been applied to the data sets to identify the final state particles. All combinations of charged pions and kaons are still included, because the event selection is the same for all $B^\pm \to h^+h^+h^-$ due to similar kinematics. Therefore, additional information from the particle identification system [19] of the detector, in particular the RICH detectors, must be used to distinguish pions from kaons. In this way, the respective

Variable	Selection cut
Transvers momentum of the track (p_{T})	$> 0.1\,\mathrm{GeV}/c$
Sumed p_{T} of the tracks	$> 4.5\,\mathrm{GeV}/c$
Momentum of the track (p)	$> 1.5\,\mathrm{GeV}/c$
Mass of the $B^{\pm}$ candidate ($M(K^{\pm}K^{+}K^{-})$) under the assumption all tracks are $K^{\pm}$	$5.05 < M_{KKK} < 6.30\,\mathrm{GeV}/c^2$
χ^2_{IP} of the individual tracks	> 1
sum of the χ^2_{IP} of all tracks	> 500
$B^{\pm}$ candidate vertex fit χ^2	< 12

Table 1: The main preselection cuts in the dataset (more details in the text).

decay channels can be studied individually. Even after this assignment, a significant fraction of misidentified particles will remain, since this process can only give probabilities for a particular type of particle and thus is not error-free. Furthermore, it is important to maintain a high efficiency in the selection of signal candidates. That is, one wants to keep as much signal as possible in one's dataset and discard as much background as possible.

Tasks:

1. Select the decay channel of interest by using the information from the particle identification system.
2. Calculate the invariant mass of the $B^{\pm}$ mesons on the real data using the correct mass hypothesis. Describe the differences from the mass distribution on simulated data. Distinguish in the plot the mass regions dominated by signal (background) events.

5.4 Global *CP*-asymmetry

The *CP*-asymmetry A_{CP} is defined by:

$$A_{\mathrm{CP}} = \frac{N^{-} - N^{+}}{N^{-} + N^{+}}. \tag{3}$$

Here N^{+} is the number of observed $B^{+} \to h^{+}h^{+}h^{-}$ events in the studied decay channel and N^{-} is the number of corresponding B^{-} decays.

Some effects can cause an apparent *CP* asymmetry. The LHC is a proton-proton collider. Therefore, the ground state in the collisions is not matter-antimatter symmetric, since protons contain only valence quarks, but not antiquarks. Such a production asymmetry would not be present, if proton and antiproton beams would collide at the LHC. Although $b\bar{b}$ quark pairs are produced in the primary production mechanism of B mesons, this still results in small production asymmetry. This amounts to about 1%. In addition, the LHCb detector may detect final-state particles with varying efficiency, as they are deflected by the magnetic field into different regions depending on their charge. This effect should be compensated for by occasionally reversing the polarity of the magnetic field. Another reason for this may be a charge-dependent interaction probability with the detector material. This is a consequence of the fact that the detector is made of matter, not antimatter.

Tasks:

1. Calculate the global CP-asymmetry.
2. Calculate the uncertainty and the significance of the CP-asymmetry.

5.5 Dalitz plots

A three-body decay can occur either by the decay of a particle directly to the three-body final state or via an intermediate resonance. For example, the decay $B^+ \to h_1^+ h_2^+ h_3^-$ could also occur via the decay $B^+ \to h_1^+ R^0$, where R^0 is a neutral particle, which decays to $R^0 \to h_2^+ h_3^-$.

An important technique for the study of three-body decays is the Dalitz plot [24]. This technique exploits the fact that the kinematics of a three-body decay can be completely described by two variables. The energies and momenta of the daughter particles are not independent of each other due to the conservation of energy and momentum. In a Dalitz plot, two of the squared invariant masses from the combination of each two final state particles are usually plotted against each other. Intermediate resonances can then be seen as bands in the Dalitz plot. In this study of the decay $B^+ \to h_1^+ h_2^+ h_3^-$, the variables $M^2_{h_1^+ h_3^-}$ and $M^2_{h_2^+ h_3^-}$ are the most obvious choices. The kinematic limits of the phase space in the decay process to which a Dalitz plot is subject is shown in Figure 3. The main features of a Dalitz plot are:

- Decays that do not proceed via resonances are evenly distributed on the Dalitz plot.
- Intermediate resonances are recognizable as bands.
- The position and size of a band is related to the mass and width of the resonance.
- The spin of the resonance determines the distribution of events along the band. Spin 0 (scalar) resonances cause uniformly filled bands. Spin 1 (vector) resonances have a minimum in the band.
- The exact pattern of events in the Dalitz plot is determined by interference between the different contributing states.

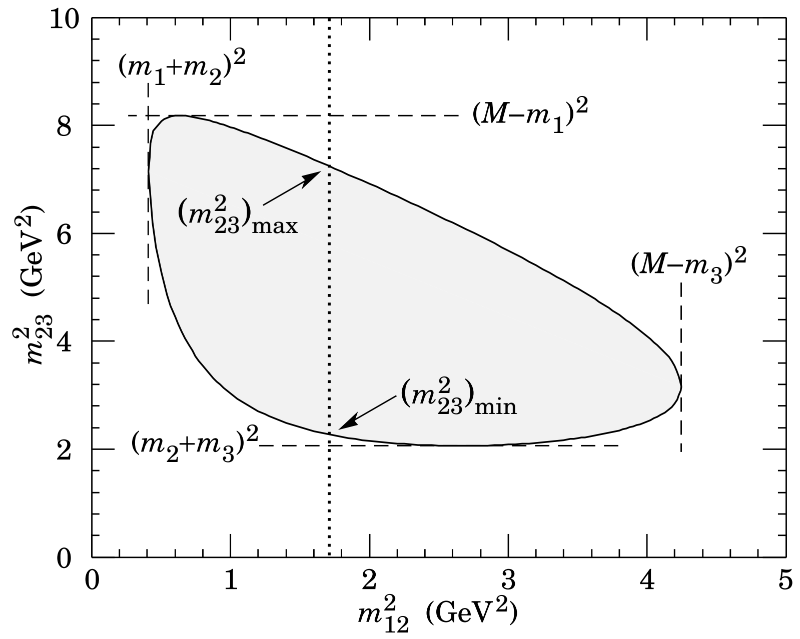

Figure 3: Dalitz plot for an example three-body final state. Four-momentum conservation constrains events to the grayed-out region. Reproduced from [23], where additional information on the technique are available.

Using the Dalitz plot, it is possible to observe and study different resonances. For the study of *CP* violation in $B^+ \to h^+h^+h^-$, it is useful to identify and remove the resonances containing c quarks. Most decays of B mesons occur in the framework of the weak interaction by a decay of the b quark into a c quark. In the region of hadrons from c quarks, *CP* violation has been observed only recently. However, the CPV is much smaller than in the b sector. A common intermediate resonance with a c quark in-B decays (B^+: $\bar{b}u$, B^0: $\bar{b}d$) is the D meson (D^+: $\bar{d}c$, D^0: $\bar{u}c$). In addition, it is also possible that the decays are $B^\pm \to J/\psi\, K^\pm$ or contain other charmonium resonances (charmonium : $c\bar{c}$).

Tasks:

1. Generate a Dalitz plot for the simulated data.
2. Generate a Dalitz plot for the experimental data.
3. Remove charm resonances.

5.6 Local *CP*-asymmetry

In section 5.4 the global *CP* asymmetry has already been calculated. However, *CP* violation originates from interference between decays over different resonances. Therefore, the *CP* asymmetry can vary in terms of sign and magnitude across phase space and, accordingly, Dalitz plot. Equation 3 can also be used to determine the CP asymmetry in local regions of phase space. Similarly, the uncertainty and significance of the asymmetry can also be determined for each of these regions. Results are considered "evidence" in particle physics at a significance greater than 3σ and "observation" or "discovery" at a significance greater than 5σ.

Tasks:

1. Create plots representing local CP violation in the area of the Dalitz plot.
2. Identifie areas with the most significant evidence of CP violation. Determine the significance in these areas and create plots that show CP asymmetry as clearly as possible.

Acknowledgements

We would like to thank our colleagues from the University of Manchester, who are pioneering the use of LHCb OpenData and have laid the groundwork for this analysis experiment.

Appendix

A Variables

The variables available for each event in the `.root` files are explained below. The data are stored in a `TTree` structure. A $B^{\pm}$ candidate is reconstructed from three charged tracks, referred to as H{1,2,3}. Not all properties have been simulated in the simulated data. Therefore, some of them contain placeholders. Not all existing variables are used in this project. However, the additional ones can be used in various extensions.

Variable	**Beschreibung**
H1_PX	Reconstucted momentum of a particle in X direction [MeV/c].
H1_PY	Reconstucted momentum of a particle in Y direction [MeV/c].
H1_PZ	Reconstucted momentum of a particle in Z direction [MeV/c]. The momentum of a particle can be reconstructed from the bend of a track in a magnetic field.
H1_ProbK	Propability that the particle is a kaon [from 0 to 1].
H1_ProbPi	Propability that the particle is a pion [from 0 to 1]. The probabilities for the different particle hypotheses are calculated based on information from RICH and the tracking detectors.
H1_Charge	Charge of the particle (+1 or -1) Determined from the direction of the bend of the particle trajectory.
H1_isMuon	Identification of a track as muon, based on information from the muon chambers (0 : false, 1 : true)
B_FlightDistance	Distance traveled of the B candidate distance between the collision point and the decay vertex determined from the three hadron tracks [mm].
B_VertexChi2	χ^2 the quality of the vertex fit of the three charged tracks.
H1_IPChi2	impact parameter (IP) χ^2.

References

[1] L. Evans and P. Bryant, *LHC Machine*, JINST **3** (2008) S08001.

[2] LHCb collaboration, A. A. Alves Jr. *et al.*, *The LHCb detector at the LHC*, JINST **3** (2008) S08005.

[3] A. Sakharov, *Violation of CP Invariance, C Asymmetry, and Baryon Asymmetry of the Universe*, Pisma Zh. Eksp. Teor. Fiz. **5** (1967) 32.

[4] J. Christenson, J. Cronin, V. Fitch, and R. Turlay, *Evidence for the 2 π Decay of the k_2^0 Meson*, Phys. Rev. Lett. **13** (1964) 138.

[5] M. Kobayashi and T. Maskawa, *CP Violation in the Renormalizable Theory of Weak Interaction*, Prog. Theor. Phys. **49** (1973) 652.

[6] BaBar, Belle, A. Bevan *et al.*, *The Physics of the B Factories*, Eur. Phys. J. **C74** (2014), no. 11 3026, `arXiv:1406.6311`.

[7] B. R. Martin and G. Shaw, *Particle physics*, Wiley-Blackwell, 2008.

[8] M. S. Sozzi, *Discrete symmetries and CP violation: From experiment to theory*, .

[9] ATLAS collaboration, G. Aad *et al.*, *Observation of a new particle in the search for the Standard Model Higgs boson with the ATLAS detector at the LHC*, Phys. Lett. **B716** (2012) 1, `arXiv:1207.7214`.

[10] CMS collaboration, S. Chatrchyan *et al.*, *Observation of a new boson at a mass of 125 GeV with the CMS experiment at the LHC*, Phys. Lett. **B716** (2012) 30, `arXiv:1207.7235`.

[11] LHCb collaboration, *LHCb Public Page*, `http://lhcb-public.web.cern.ch/lhcb-public/`, 2014. [Online; accessed 27-May-2014].

[12] LHCb collaboration, *LHCb-UK Public Page*, `www.lhcb.ac.uk/`, 2014. [Online; accessed 27-May-2014].

[13] LHCb collaboration, R. Aaij *et al.*, *Measurement of CP violation in the phase space of $B^{\pm} \to K^+K^-\pi^{\pm}$ and $B^{\pm} \to \pi^+\pi^-\pi^{\pm}$ decays*, Phys. Rev. Lett. **112** (2014) 011801, `arXiv:1310.4740`.

[14] LHCb collaboration, R. Aaij *et al.*, *Measurement of CP violation in the phase space of $B^{\pm} \to K^{\pm}\pi^+\pi^-$ and $B^{\pm} \to K^{\pm}K^+K^-$ decays*, Phys. Rev. Lett. **111** (2013) 101801, `arXiv:1306.1246`.

[15] LHCb, R. Aaij *et al.*, *LHCb Detector Performance*, Int. J. Mod. Phys. **A30** (2015) 1530022, `arXiv:1412.6352`.

[16] LHCb collaboration, R. Aaij *et al.*, *First Evidence for the Decay $B_s^0 \to \mu^+\mu^-$*, Phys. Rev. Lett. **110** (2013) 021801, `arXiv:1211.2674`.

[17] LHCb VELO Group, R. Aaij *et al.*, *Performance of the LHCb Vertex Locator*, JINST **9** (2014) 09007, `arXiv:1405.7808`.

[18] LHCb Outer Tracker group, R. Arink *et al.*, *Performance of the LHCb Outer Tracker*, JINST **9** (2014) 01002, `arXiv:1311.3893`.

[19] LHCb collaboration, M. Adinolfi *et al.*, *Performance of the LHCb RICH detector at the LHC*, Eur. Phys. J. **C73** (2013) 2431, `arXiv:1211.6759`.

[20] F. Archilli *et al.*, *Performance of the Muon Identification at LHCb*, JINST **8** (2013) P10020, `arXiv:1306.0249`.

[21] R. Aaij *et al.*, *The LHCb Trigger and its Performance in 2011*, JINST **8** (2013) P04022, `arXiv:1211.3055`.

[22] CERN, *ROOT*, `root.cern.ch/`, 2014. [Online; accessed 27-May-2014].

[23] Particle Data Group, K. Olive *et al.*, *Review of Particle Physics*, Chin. Phys. **C38** (2014) 090001.

[24] R. Dalitz, *On the analysis of tau-meson data and the nature of the tau-meson*, Phil. Mag. **44** (1953) 1068.